Electronic Supplementary Information

Spherical Co_3S_4 grown directly on Ni-Fe sulfides as porous nanoplate array on $FeNi_3$ foam: A highly efficient and durable bifunctional catalyst for Overall Water Splitting

Jun Shen[1], Qin Li[1], Wenxiu Zhang[1], Zhenyu Cai[1], Liang Cui[2], Xiuping Liu[2*], Jingquan Liu[1,2*]

[1]*College of Materials Science and Engineering, Institute for Graphene Applied Technology Innovation, Qingdao University, Qingdao, 266071, China.*

[2]*College of Materials Science and Engineering, Linyi University, Linyi, 276000 Shandong, China*

*Corresponding authors.

E-mails: lxpxin@163.com (Xiuping Liu), jliu@qdu.edu.cn (Jingquan Liu)

Experimental section

Preparation of Pt/C and RuO_2 electrodes

5 mg of Pt/C was mixed with 450 μL of deionized water, 450 μL of absolute ethanol, and 20 μL of Nafion (5 wt%), and the resulting mixture was sonicated for 60 min to obtain Pt/C ink. RuO_2 ink was prepared using the same method. Then use a pipette to draw 2 μL ink each time, which was carefully dropped onto the $FeNi_3$ foam and then dried naturally at room temperature. The total ink added was 50 μL, which was dropped in 25 times for the coating. Using this method, Pt/C electrodes and RuO_2 electrodes were prepared separately. The loading of Pt/C and RuO_2 on $FeNi_3$ foam are 1.08 mg cm^{-2}.

Electrochemical impedance spectroscopy (EIS)

In order to perform a more comprehensive test of the material, the EIS test of the electrode material was carried out under the operating conditions of OER. The test voltage applied to the material ranges from 100 kHz to 10 mHz.

Effective electrode surface area (ECSA) calculation

In order to fully demonstrate the excellent properties of the material, the ECSA of the material was estimated. In a 1.0 M KOH electrolyte solution, the material was subjected to 10 CV cycles in a voltage window from -0.15V to -0.25V vs. RHE. The test was carried out to obtain cyclic voltammograms (CVs) of the material. The electrochemical double layer capacitor (C_{dl}) of the material under the non-Faradaic overpotential, it can be obtained by CV at different scanning rates (10 mV s^{-1}, 20 mV s^{-1}, 30 mV s^{-1}, 40 mV s^{-1} and 50 mV s^{-1}). The difference in current density between

the anodic and cathodic sweeps is linear with the scan rate. A linear relationship between the two is obtained by plotting, and then the slope is obtained by data fitting, which is twice the C_{dl}. Then the ECSA of the material can be estimated by Eqn. S1:

$$ECSA = C_{dl}/C_s \qquad \text{Eqn. S1}$$

where C_s is the specific capacitance, whose value is reported to be 0.040 mF cm^{-2} in 1.0 M KOH[1].

Electrochemical contrast test

Pure graphite rods (6 mm in diameter, 99.999% purity trace metals basis) were obtained from Gaoss Union (Tianjin) Optoelectronics Technology Co., Ltd. Under other conditions unchanged, the pure graphite rods electrode (6 mm in diameter) was used instead of the Pt electrode, and the HER test was carried out on this catalyst $NiFeCoS_x@FeNi_3$. And the OER tests of synthetic material $NiFeCoS_x@FeNi_3$ in 1.0 M KOH solution with a scanning rate of 10 mV s^{-1}, 5 mV s^{-1}, 2 mV s^{-1} and 1 mV s^{-1}.

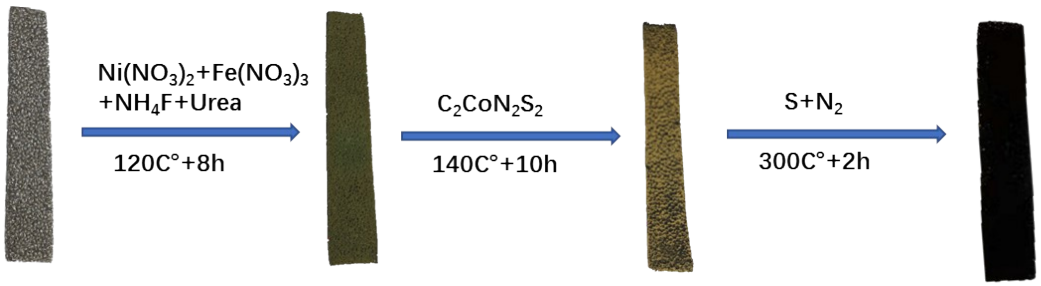

Fig. S1 Photograph of $FeNi_3$ (first left); NiFe LDH@$FeNi_3$ (second from left); NiFeCo LTHs@$FeNi_3$(third from the left) and NiFeCoS_x@$FeNi_3$ (right).

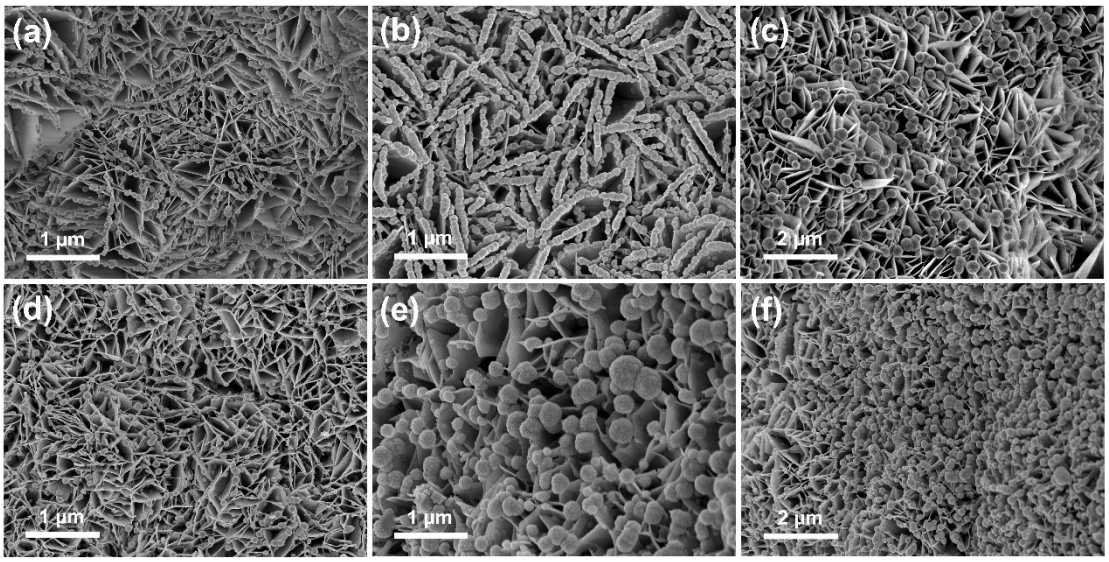

Fig. S2 SEM images of (a-c) NiFeCo LTHs@ $FeNi_3$, (d-f) $NiFeCoS_x$@$FeNi_3$.

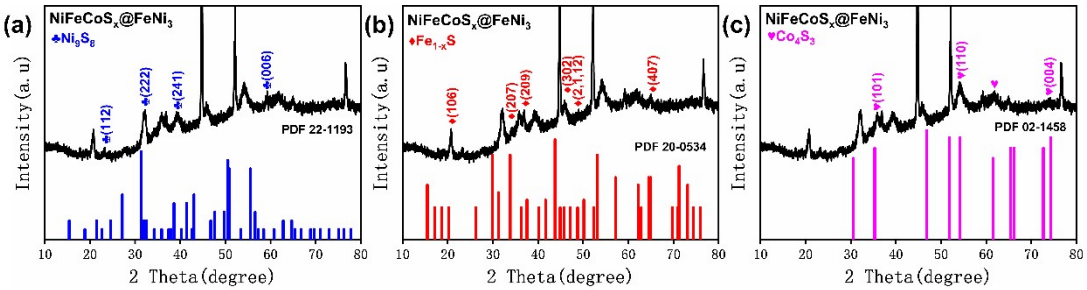

Fig. S3 XRD patterns of (a) Ni_9S_8, (b) $Fe_{1-x}S$, (c) Co_4S_3.

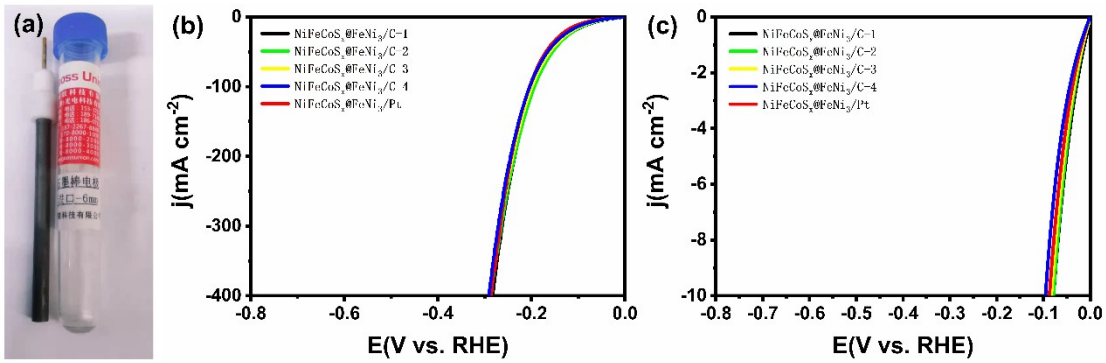

Fig. S4 (a) the pure carbon rod electrode (6 mm in diameter, 99.999% purity trace metals basis), (b) and (c) Polarization LSV curves for HER at a scan rate of 5 mV s^{-1} (iR-corrected).

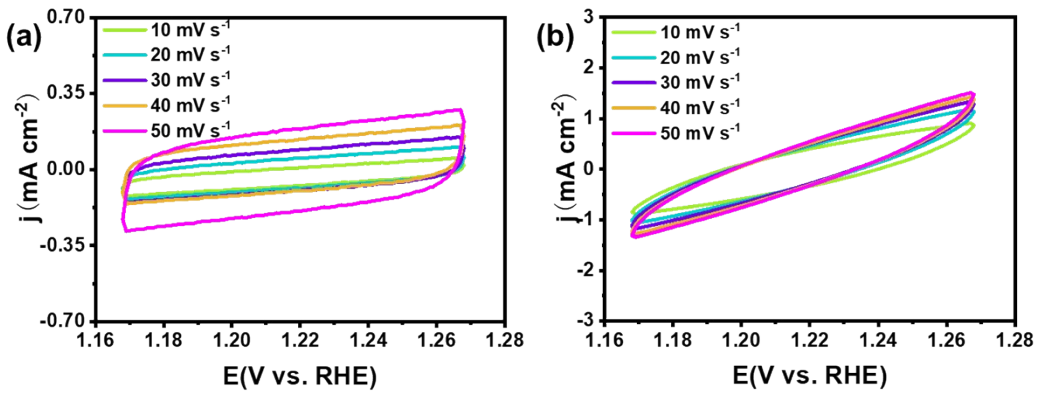

Fig. S5 Cyclic voltammograms (CVs) for (a) NiFe LDH@$FeNi_3$ and (b) NiFeCo LTHs@$FeNi_3$ at scan rates of 10, 20, 30, 40 and 50 mV s^{-1}.

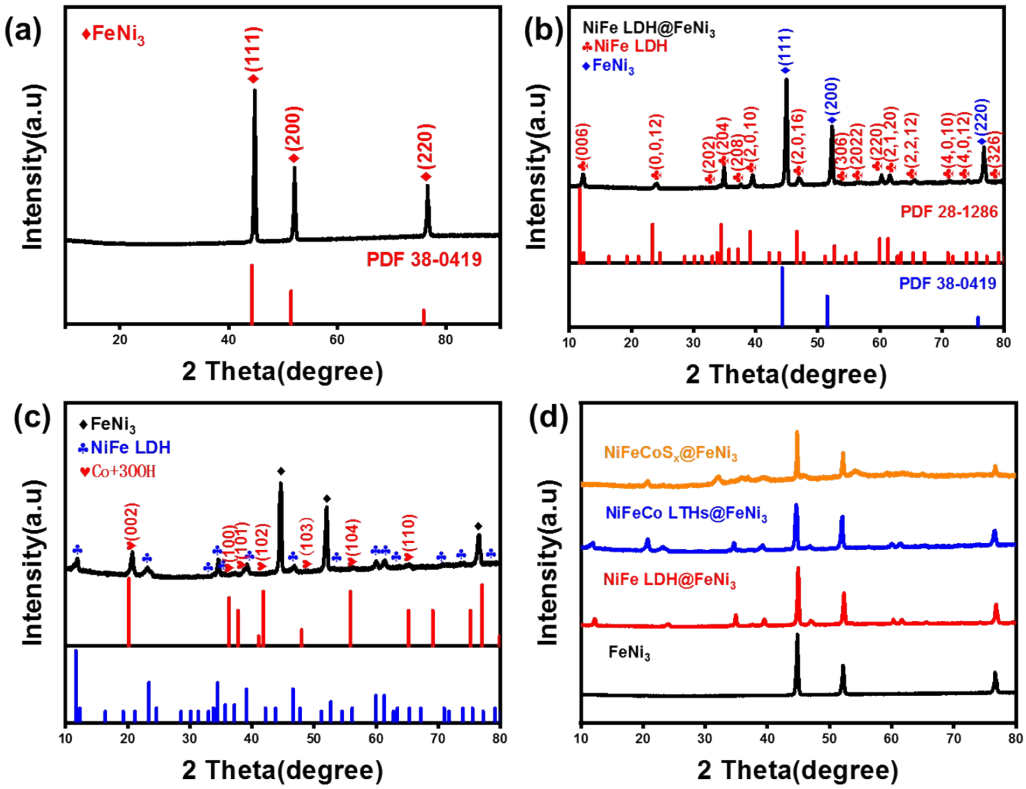

Fig. S6 XRD patterns of (a) $FeNi_3$, (b) NiFe LDH@$FeNi_3$, (c) NiFeCo LTHs@$FeNi_3$, (d) $FeNi_3$, NiFe LDH@$FeNi_3$, NiFeCo LTHs@$FeNi_3$ and $NiFeCoS_x$@$FeNi_3$.

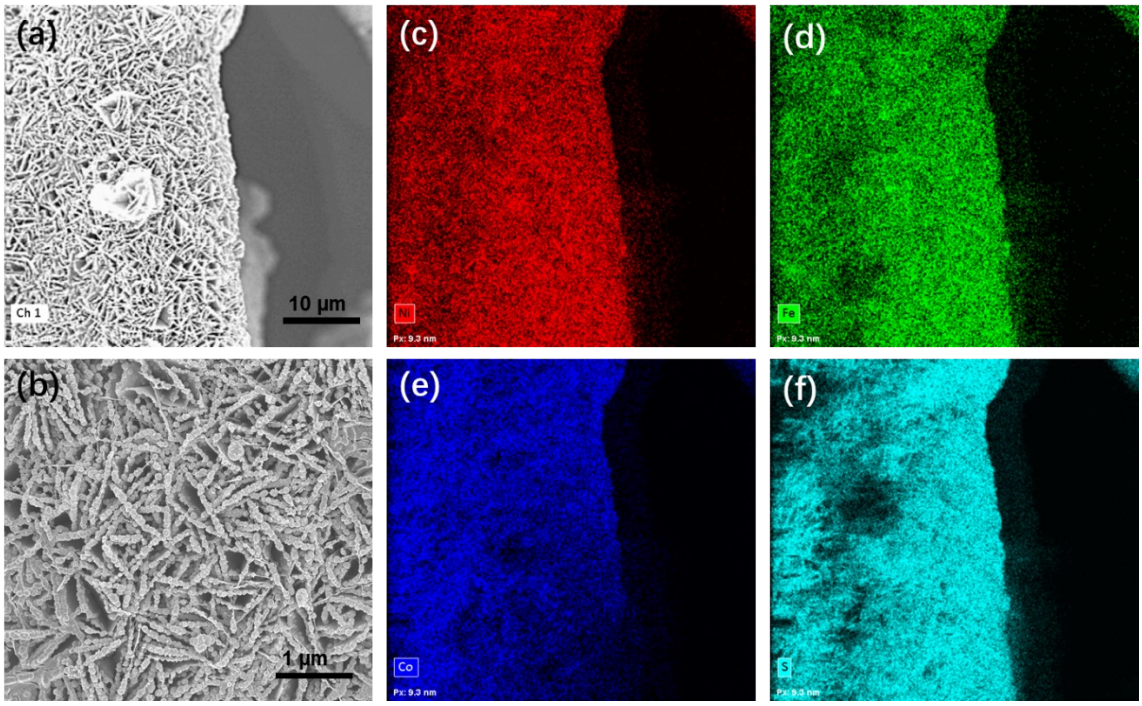

Fig. S7 (a-b) SEM image of $NiFeCoS_x$@$FeNi_3$. (c-f) the corresponding elemental mapping images of Fe, Ni, Co and S in $NiFeCoS_x$@$FeNi_3$.

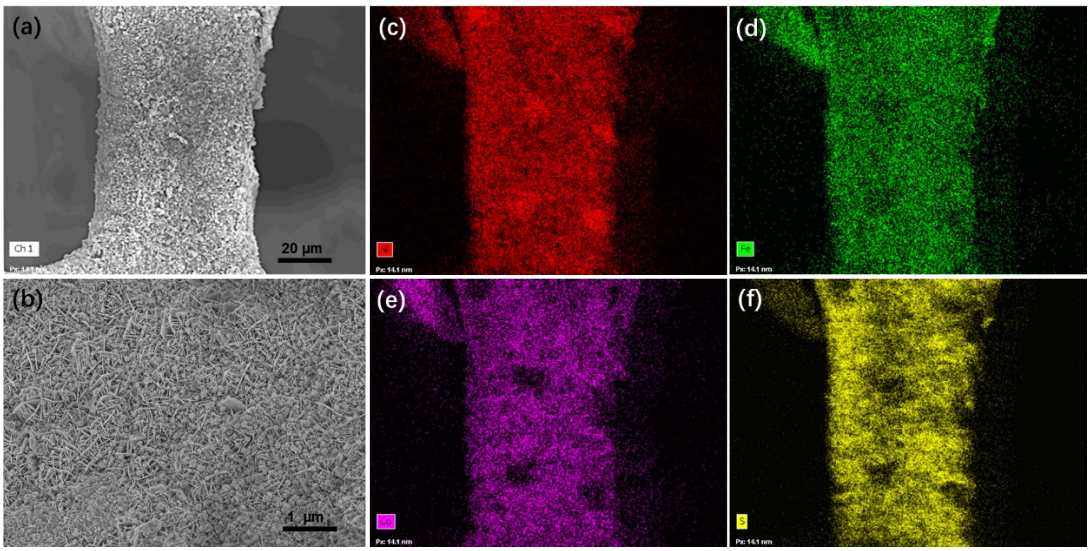

Fig. S8 (a-b) SEM image of $NiFeCoS_x$@$FeNi_3$ and (c-f) the corresponding elemental mapping images of Ni, Fe, Co and S in $NiFeCoS_x$@$FeNi_3$ after 90 h long-term stability test for OER in 1.0 M KOH solution.

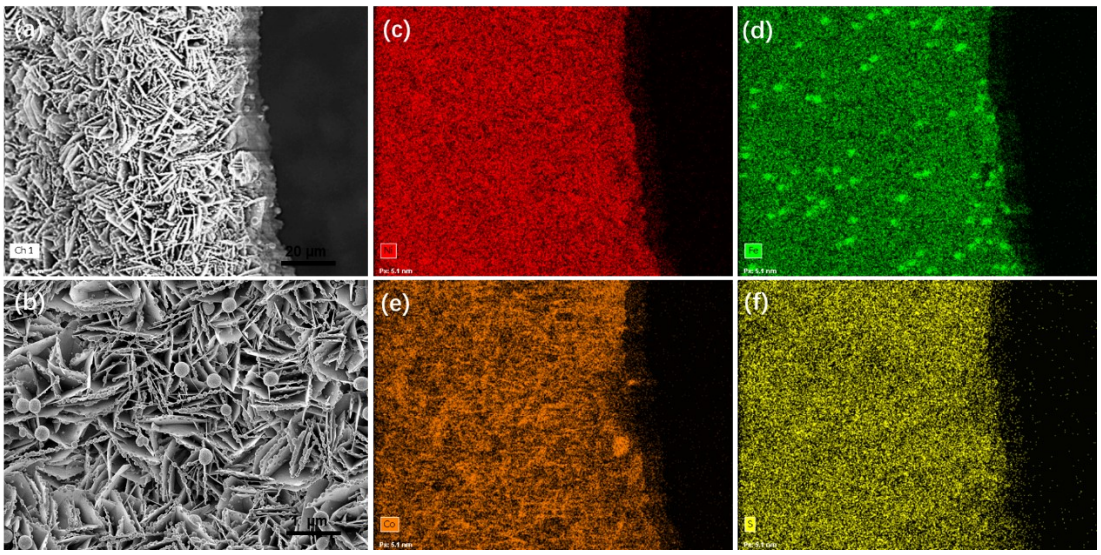

Fig. S9 (a-b) SEM image of $NiFeCoS_x$@$FeNi_3$ and (c-f) the corresponding elemental mapping images of Ni, Fe, Co and S in $NiFeCoS_x$@$FeNi_3$ after 40 h long-term stability test for HER in 1.0 M KOH solution.

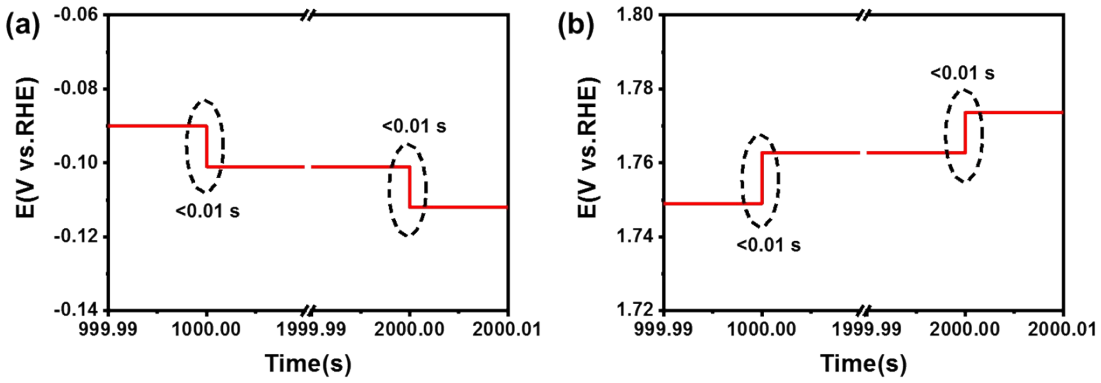

Fig. S10 The response time of (a) HER and (b) OER in the potential transition of ISTEP in 1.0 M KOH solution.

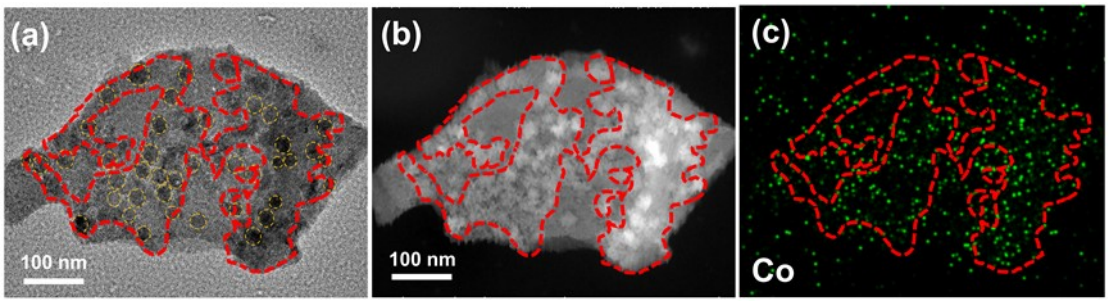

Fig. S11 The marked diagram of the scattered areas of the Co element for (a)TEM image of $NiFeCoS_x$@$FeNi_3$, (b) HAADF-STEM image of $NiFeCoS_x$@$FeNi_3$ and (c) the corresponding elemental mapping images of Co in $NiFeCoS_x$@$FeNi_3$.

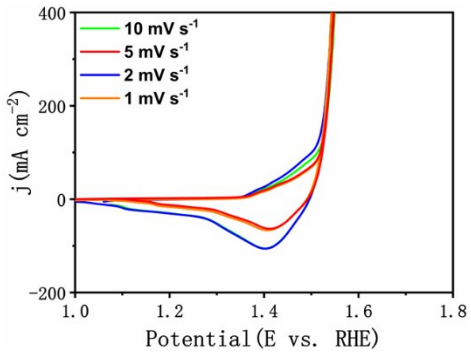

Fig. S12 The OER polarisation LSV curves for $NiFeCoS_x$@$FeNi_3$ with scan rates of 10 mV s^{-1}, 5 mV s^{-1}, 2 mV s^{-1} and 1 mV s^{-1} (iR-corrected).

Table S1 The comparison of catalytic performances for HER between $NiFeCoS_x$@$FeNi_3$ and other materials reported in the literature.

Catalyst	Overpotential	Tafel slope	Electrolyte	Reference
$NiFeCoS_x$@$FeNi_3$	88@10	116	1M KOH	This work
NiFeCo LTHs@$FeNi_3$	112@10	187	1M KOH	This work
NiFe LDH@$FeNi_3$	168@10	194	1M KOH	This work
(Ni,Fe)S_2/MoS_2	130@10	101.22	1M KOH	[2]
$FeCo_2S_4$	132@10	164	1M KOH	[3]
NiCo/$NiCo_2S_4$/NiCo/Ni	132@10	58.2	1M KOH	[4]
$Ni_xCo_{3-x}S_4$/Ni_3S_2/NF	136@10	107	1M KOH	[1]
Sn-Ni_3S_2/NF	137@10	148	1M KOH	[5]
NiCoFe LTHs/CFC	200@10	70	1M KOH	[6]
NiFeS/NF	180@10	53	1M KOH	[7]
V−Ni_3S_2−NW	203@20	112	1M KOH	[8]
Ni-Co-S	228@10	101.76	1M KOH	[9]
$(Fe_{0.5}Ni_{0.5})S_2$	250@10	115.9	1M KOH	[10]

Table S2 The comparison of catalytic performances for OER between $NiFeCoS_x$@$FeNi_3$ and other materials reported in the literature.

Catalyst	Overpotential (mV)	Tafel slope (mV dec^{-1})	Electrolyte	Reference
$NiFeCoS_x$@$FeNi_3$	210@10	45	1M KOH	This work
NiFeCo LTHs@$FeNi_3$	275@10	68	1M KOH	This work
NiFe LDH@$FeNi_3$	380@10	172	1M KOH	This work
Ni_3S_2/$Co(OH)_2$	257@10	63.1	1M KOH	[11]
$NiCo_2S_4$ NW/NF	260@10	40	1M KOH	[12]
Ni-Co-S	270@40	133.8	1M KOH	[13]
$(Fe_{0.5}Ni_{0.5})S_2$	270@10	74.41	1M KOH	[10]
(Ni,Fe)S_2/MoS_2	270@10	43.21	1M KOH	[14]
Fe-Co_9S_8 NM	270@10	70	1M KOH	[15]
Ni-Co-P-S	280@10	69	1M KOH	[16]
Fe-Ni-O_x/GC	286@10	48	1M KOH	[17]
$LiCo_{0.33}Ni_{0.33}Fe_{0.33}O_2$/GC	295@10	46	1M KOH	[18]
$FeNiS_2$ NSs	310@10	46	1M KOH	[19]
NiCoFe LTHs/CFC	240@10	32	1M KOH	[6]
NiCoFe LDHs	275@10	52	1M KOH	[20]

Table S3 The value of C_{dl} for different catalysts in 1.0 M KOH solution.

Samples	C_{dl} (mF cm^{-2})	Reference
$NiFeCoS_x$@$FeNi_3$	248	This work
NiFeCo LTHs@$FeNi_3$	46.9	This work
NiFe LDH@$FeNi_3$	3	This work
Co_4S_3-NiCo LDH/CC	7.36	[21]
$(Ni_{0.5}Fe_{0.5})_2P$	5.5	[22]
Y-S Ni-Co-Se/CFP	8	[23]
CoS_x/Ni_3S_2@NF	8.68	[24]
$Co_{0.7}Fe_{0.3}P_3$	11.3	[25]
CoP-Co_2P@PC/PG NHs	23.5	[26]
Co-CoO_x@CN	29.6	[27]
Co_9S_8@Co_3O_4	38	[28]

References

[1] Y. Wu, Y. Liu, G. Li, X. Zou, X. Lian, D. Wang, L. Sun, T. Asefa, X. Zou, Efficient electrocatalysis of overall water splitting by ultrasmall $Ni_xCo_{3-x}S_4$ coupled Ni_3S_2 nanosheet arrays, Nano Energy, 35 (2017) 161-170.

[2] Y. Liu, S. Jiang, S. Li, L. Zhou, Z. Li, J. Li, M. Shao, Interface engineering of (Ni, Fe)S_2@MoS_2 heterostructures for synergetic electrochemical water splitting, Applied Catalysis B-Environmental, 247 (2019) 107-114.

[3] J. Hu, Y. Ou, Y. Li, D. Gao, Y. Zhang, P. Xiao, $FeCo_2S_4$ Nanosheet Arrays Supported on Ni Foam: An Efficient and Durable Bifunctional Electrocatalyst for Overall Water-Splitting, ACS Sustain. Chem. Eng., 6 (2018) 11724-11733.

[4] Y. Ning, D. Ma, Y. Shen, F. Wang, X. Zhang, Constructing hierarchical mushroom-like bifunctional NiCo/$NiCo_2S_4$@NiCo/Ni foam electrocatalysts for efficient overall water splitting in alkaline media, Electrochim. Acta, 265 (2018) 19-31.

[5] J. Yu, F.-X. Ma, Y. Du, P.-P. Wang, C.-Y. Xu, L. Zhen, In Situ Growth of Sn-Doped Ni_3S_2 Nanosheets on Ni Foam as High-Performance Electrocatalyst for Hydrogen Evolution Reaction, Chemelectrochem, 4 (2017) 594-600.

[6] L. Qian, Z. Lu, T. Xu, X. Wu, Y. Tian, Y. Li, Z. Huo, X. Sun, X. Duan, Trinary Layered Double Hydroxides as High-Performance Bifunctional Materials for Oxygen Electrocatalysis, Advanced Energy Materials, 5 (2015).

[7] S. Shanmugam, P. Ganesan, A. Sivanantham, Inexpensive electrochemical synthesis of nickel iron sulphides on nickel foam: Super active and ultra-durable

electrocatalysts for alkaline electrolyte membrane water electrolysis, J. Mater. Chem. A, (2016).

[8] Y. Qu, M. Yang, J. Chai, Z. Tang, M. Shao, C.T. Kwok, M. Yang, Z. Wang, D. Chua, S. Wang, Z. Lu, H. Pan, Facile Synthesis of Vanadium-Doped Ni_3S_2 Nanowire Arrays as Active Electrocatalyst for Hydrogen Evolution Reaction, ACS Appl. Mater. Interfaces, 9 (2017) 5959-5967.

[9] D. Zhang, W. He, Z. Zhang, X. Xu, Structure-design and synthesis of Nickel-Cobalt-Sulfur arrays on nickel foam for efficient hydrogen evolution, J. Alloys Compd., 785 (2019) 468-474.

[10] N. Xiong, S. Wang, Y. Xie, Q. Feng, X. Wang, M. Li, Z. Xu, W. Zhou, K. Pan, Multifunctional $(Fe_{0.5}Ni_{0.5})S_2$ nanocrystal catalysts with high catalytic activities for reduction of I^{3-} and electrochemical water splitting, Res. Chem. Intermed., 44 (2018) 4307-4322.

[11] S. Wang, L. Xu, W. Lu, Synergistic effect: Hierarchical Ni_3S_2@$Co(OH)_2$ heterostructure as efficient bifunctional electrocatalyst for overall water splitting, Appl. Surf. Sci., 457 (2018) 156-163.

[12] A. Sivanantham, P. Ganesan, S. Shanmugam, Hierarchical $NiCo_2S_4$ nanowire arrays supported on ni foam: An efficient and durable bifunctional electrocatalyst for oxygen and hydrogen evolution reactions, Adv. Funct. Mater., 26 (2016) 4661-4672.

[13] Y. Gong, Z. Xu, H. Pan, Y. Lin, Z. Yang, J. Wang, A 3D well-matched electrode pair of Ni–Co–S//Ni–Co–P nanoarrays grown on nickel foam as a high-performance electrocatalyst for water splitting, J. Mater. Chem. A, 6 (2018) 12506-12514.

[14] Y. Liu, S. Jiang, S. Li, L. Zhou, Z. Li, J. Li, M. Shao, Interface engineering of (Ni, Fe)S_2@MoS_2 heterostructures for synergetic electrochemical water splitting, Appl. Catal., B, 247 (2019) 107-114.

[15] W. Gao, J. Qin, K. Wang, K. Yan, Z. Liu, J. Lin, Y. Chai, C. Liu, B. Dong, Facile synthesis of Fe-doped Co_9S_8 nano-microspheres grown on nickel foam for efficient oxygen evolution reaction, Appl. Surf. Sci., 454 (2018) 46-53.

[16] Y. Tian, Z. Lin, J. Yu, S. Zhao, Q. Liu, J. Liu, R. Chen, Y. Qi, H. Zhang, R. Li, J. Li, J. Wang, Superaerophobic Quaternary Ni–Co–S–P Nanoparticles for Efficient Overall Water-Splitting, ACS Sustain. Chem. Eng., 7 (2019) 14639-14646.

[17] L. Kuai, J. Geng, C. Chen, E. Kan, Y. Liu, Q. Wang, B. Geng, A Reliable Aerosol-Spray-Assisted Approach to Produce and Optimize Amorphous Metal Oxide Catalysts for Electrochemical Water Splitting, Angew. Chem. Int. Ed., 53 (2014) 7547-7551.

[18] Z. Lu, H. Wang, D. Kong, K. Yan, P. Hsu, G. Zheng, H. Yao, Z. Liang, X. Sun, Y. Cui, Electrochemical tuning of layered lithium transition metal oxides for improvement of oxygen evolution reaction, Nat. Commun., 5 (2014) 4345.

[19] J. Jiang, S. Lu, H. Gao, X. Zhang, H. Yu, Ternary $FeNiS_2$ ultrathin nanosheets as an electrocatalyst for both oxygen evolution and reduction reactions, Nano Energy, 27 (2016) 526-534.

[20] H. Liang, F. Meng, M. Caban-Acevedo, L. Li, A. Forticaux, L. Xiu, Z. Wang, S. Jin, Hydrothermal continuous flow synthesis and exfoliation of NiCo layered double hydroxide nanosheets for enhanced oxygen evolution catalysis, Nano Lett, 15 (2015)

1421-1427.

[21] X.Y. Zang, X. Zhang, J.X. Guo, Electrodeposition of Co4S3 on NiCo LDH nanosheet arrays for advanced hydrogen evolution, Mater. Lett., 285 (2021) 5.

[22] J. Yu, G. Cheng, W. Luo, Hierarchical NiFeP microflowers directly grown on Ni foam for efficient electrocatalytic oxygen evolution, J. Mater. Chem. A, 5 (2017) 11229-11235.

[23] K. Ao, J. Dong, C. Fan, D. Wang, Y. Cai, D. Li, F. Huang, Q. Wei, Formation of yolk–shelled nickel–cobalt selenide dodecahedral nanocages from metal–organic frameworks for efficient hydrogen and oxygen evolution, ACS Sustain. Chem. Eng., 6 (2018) 10952-10959.

[24] S. Shit, S. Chhetri, W. Jang, N.C. Murmu, H. Koo, P. Samanta, T. Kuila, Cobalt Sulfide/Nickel Sulfide Heterostructure Directly Grown on Nickel Foam: An Efficient and Durable Electrocatalyst for Overall Water Splitting Application, ACS Appl. Mater. Inter., 10 (2018) 27712-27722.

[25] L. Lin, Q. Fu, Y. Han, J. Wang, X. Zhang, Y. Zhang, C. Hu, Z. Liu, Y. Sui, X. Wang, Fe doped skutterudite-type CoP_3 nanoneedles as efficient electrocatalysts for hydrogen and oxygen evolution in alkaline media, J. Alloys Compd., 808 (2019) 151767.

[26] J. Yang, D. Guo, S. Zhao, Y. Lin, R. Yang, D. Xu, N. Shi, X. Zhang, L. Lu, Y.Q. Lan, J. Bao, M. Han, Cobalt Phosphides Nanocrystals Encapsulated by P-Doped Carbon and Married with P-Doped Graphene for Overall Water Splitting, Small, 15 (2019) 1804546.

[27] H. Jin, J. Wang, D. Su, Z. Wei, Z. Pang, Y. Wang, In situ cobalt–cobalt oxide/N-doped carbon hybrids as superior bifunctional electrocatalysts for hydrogen and oxygen evolution, J. Am. Chem. Soc., 137 (2015) 2688-2694.

[28] S. Deng, S. Shen, Y. Zhong, K. Zhang, J. Wu, X. Wang, X. Xia, J. Tu, Assembling Co_9S_8 nanoflakes on Co_3O_4 nanowires as advanced core/shell electrocatalysts for oxygen evolution reaction, J. Energy Chem., 26 (2017) 1203-1209.